

Supporting Information for

***p*-Benzoquinone adsorption/separation, sensing and its photoinduced transformation within a robust Cd(II)-MOF in a SC-Sc fashion**

Fan Yang, Qi-Kui Liu,* Dan Wu, An-Yan Li, and Yu-Bin Dong*

College of Chemistry, Chemical Engineering and Materials Science, Collaborative Innovation Center of Functionalized Probes for Chemical Imaging in Universities of Shandong, Key Laboratory of Molecular and Nano Probes, Ministry of Education, Shandong Normal University, Jinan 250014, P. R. China. E-mail: yubindong@sdu.edu.cn, qikuiliu2004@163.com

Contents

Section I. Chemicals and Instruments

Section II. Figures S1-S11

Section III. Single-Crystal X-ray Crystallography

Section IV. Crystal Data (Table S1-S3)

Section I. Chemicals and Instruments

All the chemicals were obtained from commercial sources and used without further purification. Infrared (IR) spectrums were obtained in the 400-4000 cm^{-1} range using a Bruker ALPHA FT-IR Spectrometer. Elemental analyses were performed on a Perkin-Elmer model 2400 analyzer. ^1H NMR data were collected on a Bruker Avance-300 spectrometer. Chemical shifts are reported in δ relative to TMS. All crystal data were obtained by Agilent SuperNova X-Ray single crystal diffractometer. All fluorescence measurements were carried out on a Cary Eclipse spectrofluorimeter (Varian, Australia) equipped with a xenon lamp and quartz carrier at room temperature. EPR spectrums were obtained by Bruker A300 EPR Spectrometer. GC-MS analysis data were performed on a J&K S011525-300 gas chromatographic (Agilent 6890GC-5973MS). The separation data were obtained by Agilent 1260 Infinity HPLC system equipped with an Agilent C18 reverse phase column (150 \times 4.6 mm, 5 μm). Thermogravimetric analyses were carried out on a TA Instrument Q5 simultaneous TGA under flowing nitrogen at a heating rate of 10 $^\circ\text{C}/\text{min}$. XRPD patterns was obtained on D8 ADVANCE X-ray powder diffractometer with Cu K α radiation ($\lambda = 1.5405 \text{ \AA}$).

Section II. Figures S1-S11

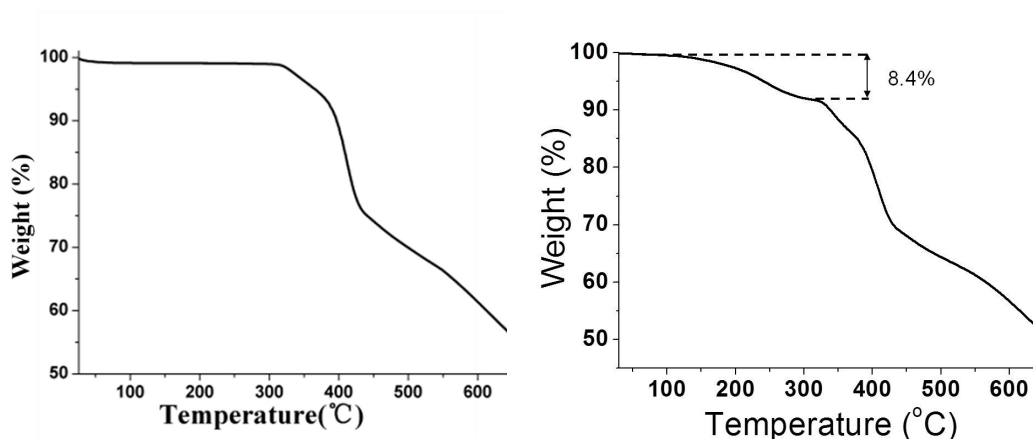


Figure S1. Left: TGA trace of $\text{H}_2\text{O} \cdot [\text{CdL}_2 \cdot (\text{ClO}_4)_2]$ (**1**). The observed water guest mass loss is 1.4 % (calculated 1.6%). Right: $\text{Q} \cdot [\text{CdL}_2 \cdot (\text{ClO}_4)_2]$ (**2**). The observed Q guest mass loss is 8.4 % (calculated 8.4%).

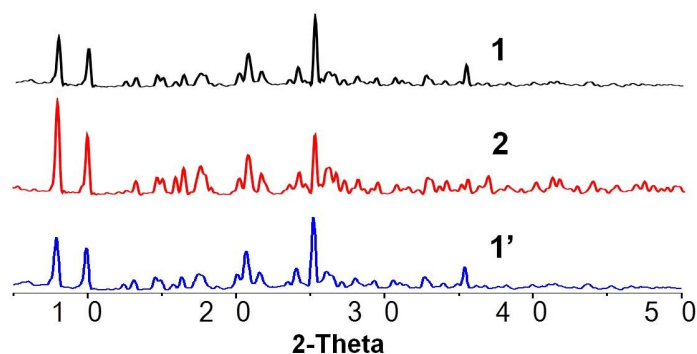


Figure S2. XRPD patterns of **1**, **2**, and regenerated of **1** (**1'**).

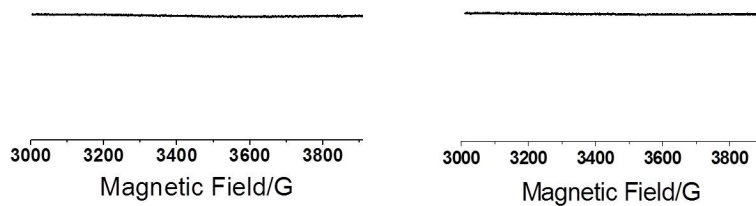


Figure S3. The ESR spectra for **Q** before (left) and after (right) exposed to simulated solar light.

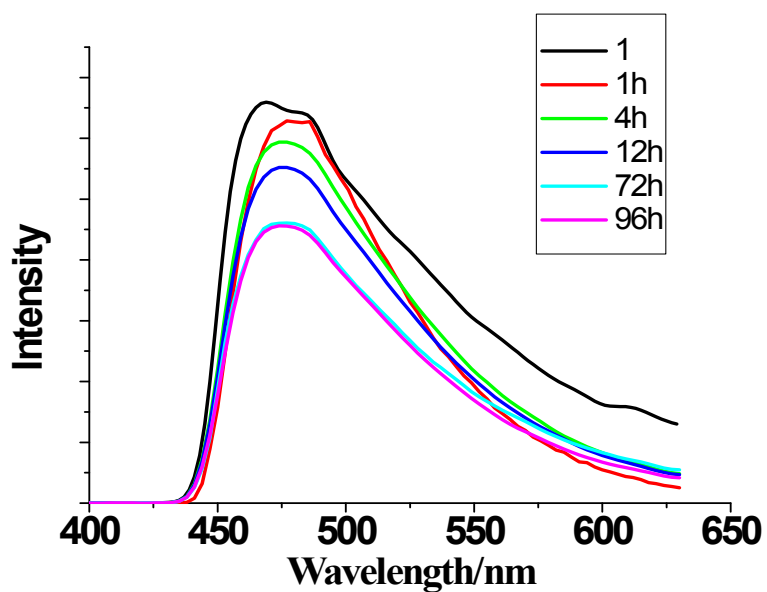


Figure S4. The solid state emission spectra of **1** recorded in an aqueous solution of **Q** (0.02 mg/L).

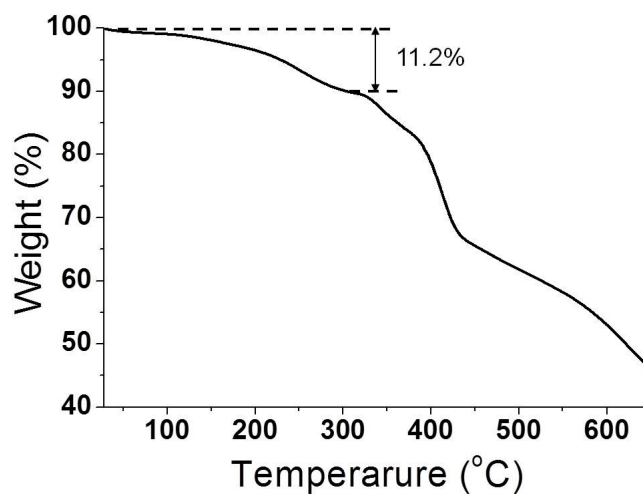


Figure S5. TGA trace of $\text{Q}/(\text{EtOH})\text{C}_2\text{D}_2(\text{ClO}_4)_2$ (**3**). The observed total **Q** and EtOH mass loss is 11.2 % (calculated 12.4%).

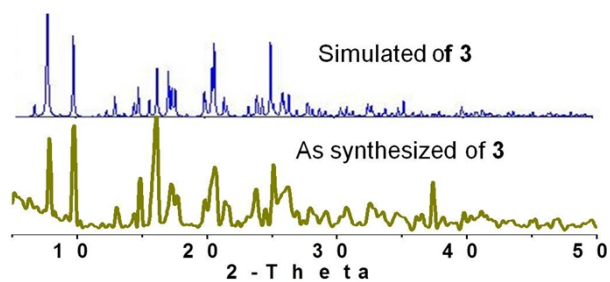


Figure S6. XRPD patterns of **3**, indicating that **3** was obtained in a pure phase.

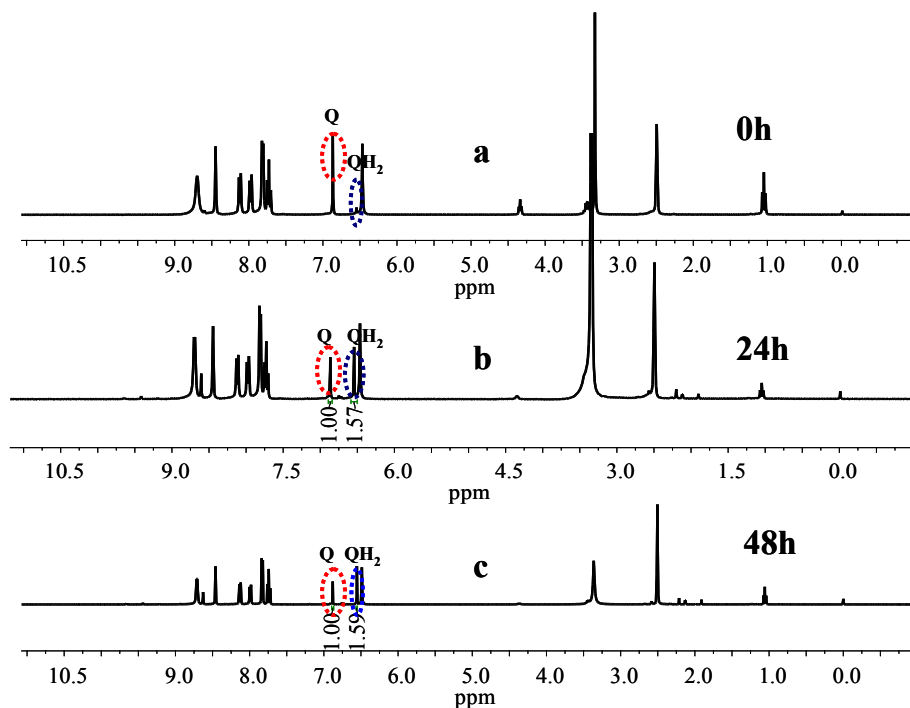
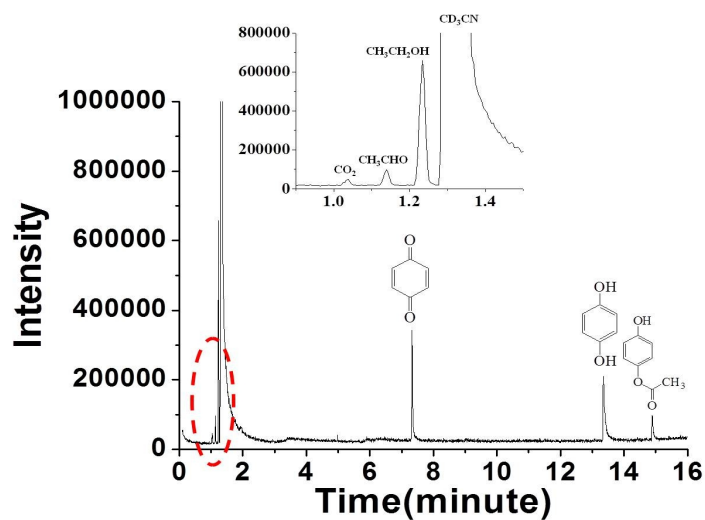


Figure S7. a) The ^1H NMR spectrum (300 MHz, $\text{DMSO}-d_6$) of **3**. b) The ^1H NMR spectrum (300 MHz, $\text{DMSO}-d_6$) of **3** exposed to simulated solar light for 24h. c) The ^1H NMR spectrum (300 MHz, $\text{DMSO}-d_6$) of **3** exposed to simulated solar light for 48h. No more conversion of **Q** can be realized over 24 h based on the ^1H NMR spectra.



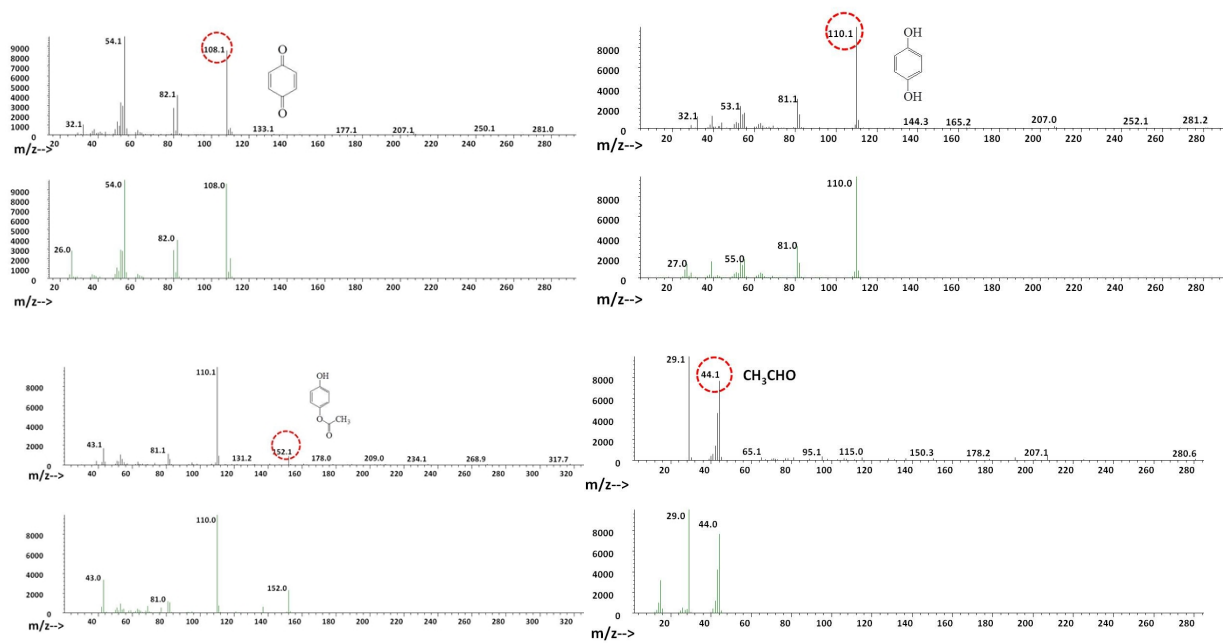
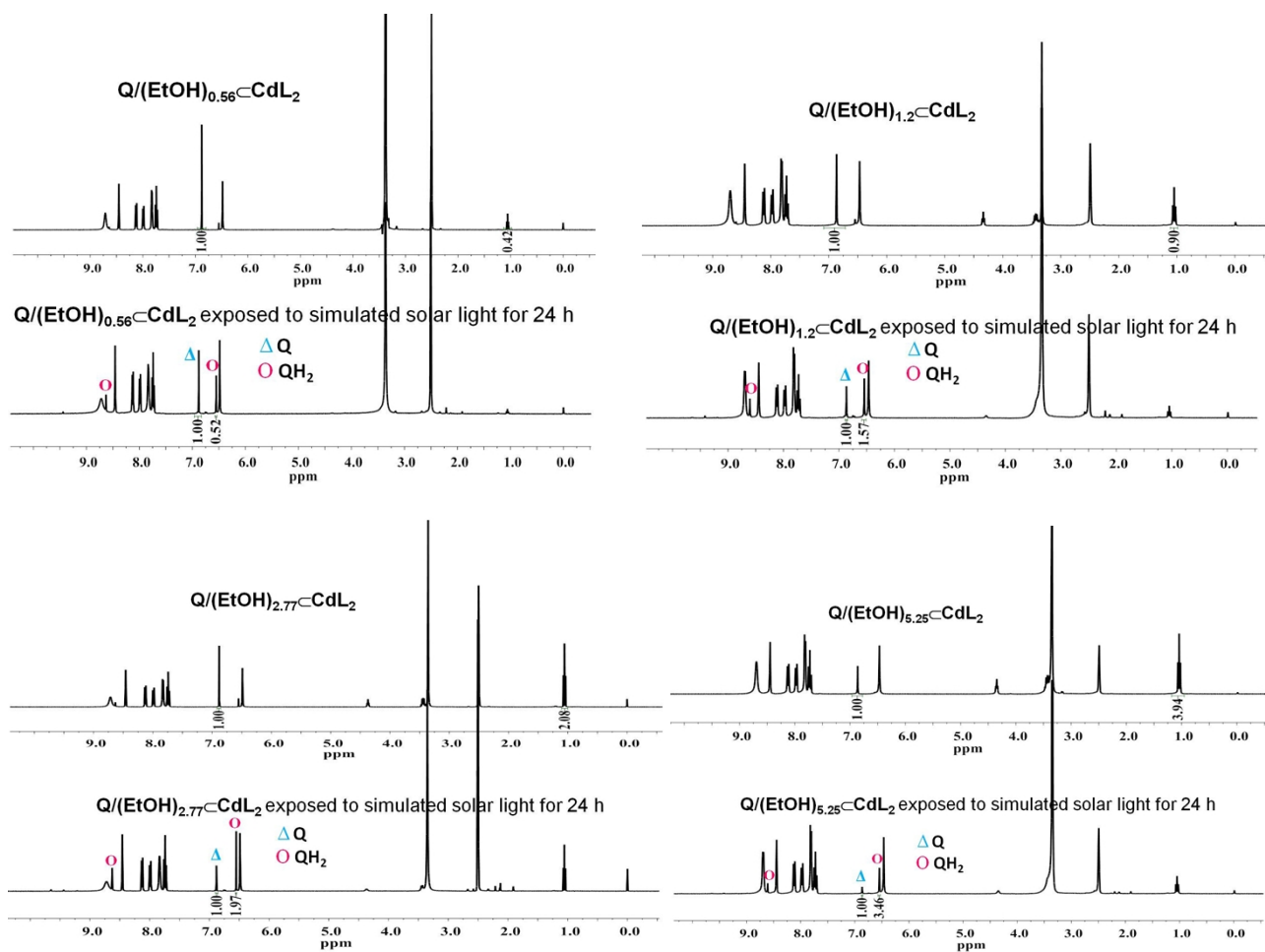


Figure S8. GC-MS analysis performed on the CH_3CN extract of **4**.



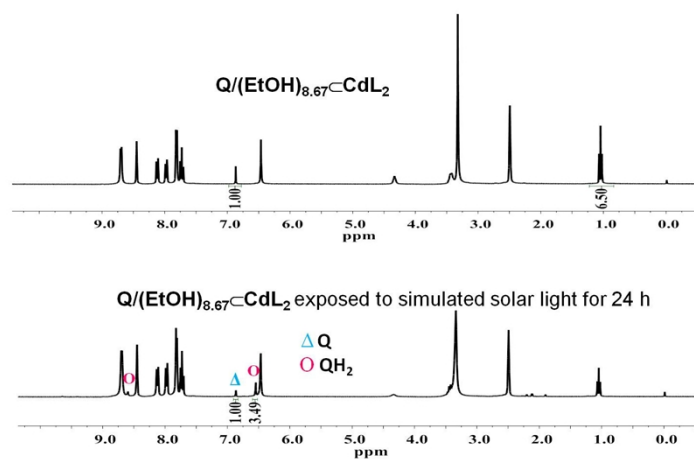
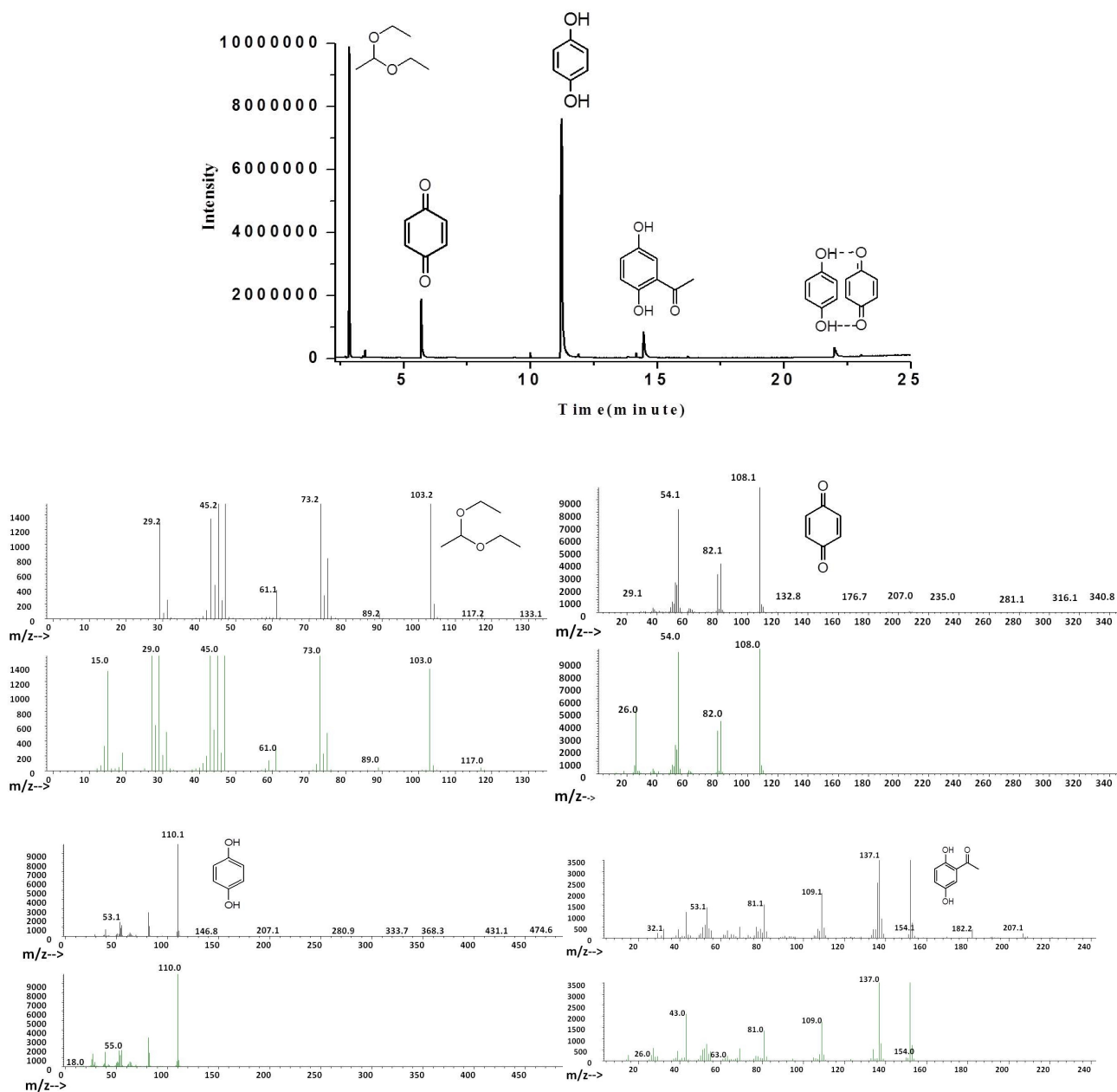


Figure S9. When the ratios of **Q**/EtOH are 1/0.56, 1/1.20, 1/2.77, 1/5.25, 1/8.67, the conversions of **Q** are 34.2, 61.0, 66.3, 77.5 and 77.7%, respectively.



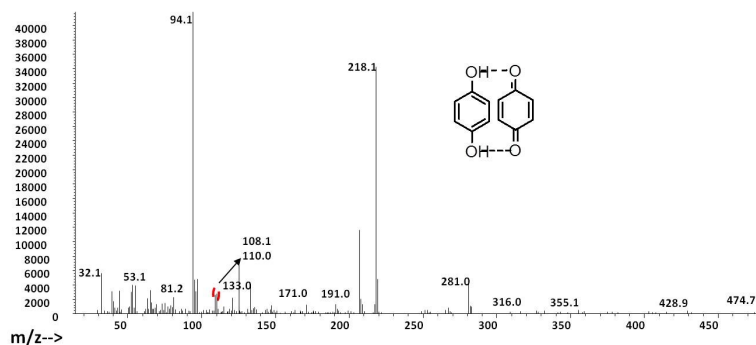


Figure S10. GC-MS analysis of photolysis of **Q** in EtOH solution.

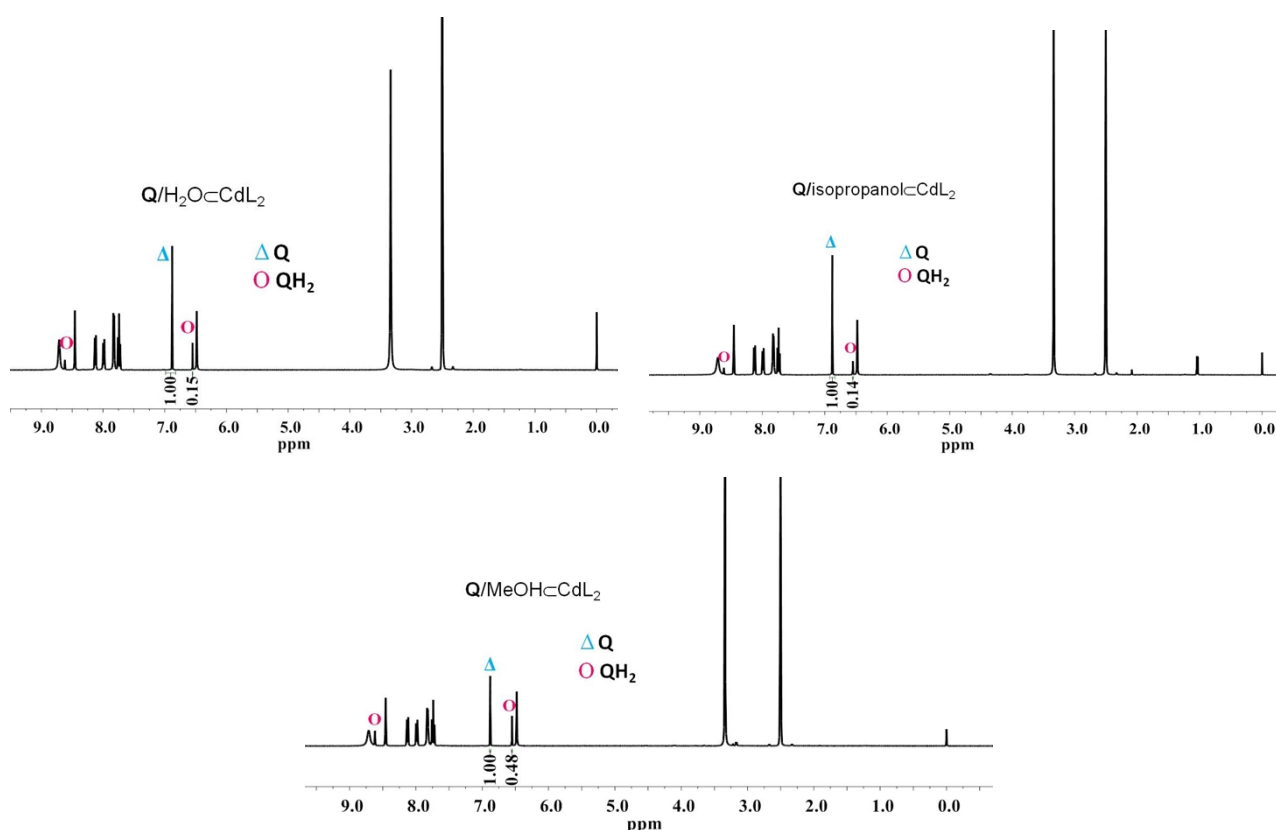


Figure S11. The conversions of **Q** within the adsorption saturated $\text{Q}/\text{H}_2\text{O} \subset \text{CdL}_2$, $\text{Q}/\text{isopropanol} \subset \text{CdL}_2$ and $\text{Q}/\text{MeOH} \subset \text{CdL}_2$ are 13.0, 12.3 and 32.4% based on ^1H NMR spectra.

Section III. Single-Crystal X-ray Crystallography

X-ray structure determination of 2. A block like crystal of **2** was epoxied onto the end of a thin glass fiber. X-ray intensity data were measured at 100 K on a Agilent SuperNova CCD-based diffractometer (Mo $K\alpha$ radiation, $\lambda = 0.71073 \text{ \AA}$).¹ After determination of crystal quality and initial tetragonal unit cell parameters, a hemi sphere of frame data was collected. The raw data frames were integrated with CrysAlisPro, Agilent Technologies, Version 1.171.36.32 (release 02-08-2013 CrysAlis171. NET) (compiled Aug 2 2013, 16 : 46 : 58).¹ Empirical absorption correction using spherical harmonics, implemented in SCALE3 ABSPACK scaling algorithm. The final unit cell parameters are based on the least-squares refinement of 5167

reflections from the data set with $I > 5\sigma(I)$. Analysis of the data showed negligible crystal decay during data collection. Systematic absences in the intensity data were consistent with the space groups $P4(3)2(1)2$. Solution and refinement in $P4(3)2(1)2$ yielded. The structure was solved by a combination of direct methods and difference Fourier syntheses, and refined by full-matrix least-squares against F^2 , using the SHELXTL software package.² All non-hydrogen atoms of the framework were refined with anisotropic displacement parameters. Hydrogen atoms were placed in geometrically idealized positions and included as standard riding atoms.

X-ray structure determination of 3. A block like crystal of **3** was epoxied onto the end of a thin glass fiber. X-ray intensity data were measured at 100 K on a Agilent SuperNova CCD-based diffractometer (Mo $K\alpha$ radiation, $\lambda = 0.71073 \text{ \AA}$).¹ After determination of crystal quality and initial tetragonal unit cell parameters, a hemi sphere of frame data was collected. The raw data frames were integrated with CrysAlisPro, Agilent Technologies, Version 1.171.36.32 (release 02-08-2013 CrysAlis171. NET) (compiled Aug 2 2013, 16 : 46 : 58).¹ Empirical absorption correction using spherical harmonics, implemented in SCALE3 ABSPACK scaling algorithm. The final unit cell parameters are based on the least-squares refinement of 5128 reflections from the data set with $I > 5\sigma(I)$. Analysis of the data showed negligible crystal decay during data collection. Systematic absences in the intensity data were consistent with the space groups $P4(3)2(1)2$. Solution and refinement in $P4(3)2(1)2$ yielded. The structure was solved by a combination of direct methods and difference Fourier syntheses, and refined by full-matrix least-squares against F^2 , using the SHELXTL software package.² All non-hydrogen atoms of the framework were refined with anisotropic displacement parameters. Hydrogen atoms were placed in geometrically idealized positions and included as standard riding atoms.

X-ray structure determination of 4. A block like crystal of **4** was epoxied onto the end of a thin glass fiber. X-ray intensity data were measured at 100 K on a Agilent SuperNova CCD-based diffractometer (Mo $K\alpha$ radiation, $\lambda = 0.71073 \text{ \AA}$).¹ After determination of crystal quality and initial tetragonal unit cell parameters, a hemi sphere of frame data was collected. The raw data frames were integrated with CrysAlisPro, Agilent Technologies, Version 1.171.36.32 (release 02-08-2013 CrysAlis171. NET) (compiled Aug 2 2013, 16 : 46 : 58).¹ Empirical absorption correction using spherical harmonics, implemented in SCALE3 ABSPACK scaling algorithm. The final unit cell parameters are based on the least-squares refinement of 5142 reflections from the data set with $I > 5\sigma(I)$. Analysis of the data showed negligible crystal decay during data collection. Systematic absences in the intensity data were consistent with the space groups $P4(1)2(1)2$. Solution and refinement in $P4(1)2(1)2$ yielded. The structure was solved by a combination of direct methods and difference Fourier syntheses, and refined by full-matrix least-squares against F^2 , using the SHELXTL software package.² All non-hydrogen atoms of the framework were refined with anisotropic displacement parameters. Hydrogen atoms were placed in geometrically idealized positions and included as standard riding atoms.

Section IV. Crystal Data (Table S1-S3)

Table S1. Crystal data and structure refinement for **2**.

Identification code	2
Empirical formula	C ₅₄ H ₄₀ CdCl ₂ N ₁₂ O ₁₀
Formula weight	1200.28
Temperature	100.0(2) K
Wavelength	0.71073 Å
Crystal system, space group	Tetragonal, <i>P 43 21 2</i>
Unit cell dimensions	a = 15.8664(4) Å alpha = 90 deg. b = 15.8664(4) Å beta = 90 deg. c = 21.7986(13) Å gamma = 90 deg.
Volume	5487.7(4) Å ³
Z, Calculated density	4, 1.453 Mg/m ³
Absorption coefficient	0.564 mm ⁻¹
F(000)	2440
Crystal size	0.29 x 0.17 x 0.08 mm
Theta range for data collection	3.02 to 25.60 deg.
Reflections collected / unique	16438 / 5167 [R(int) = 0.0401]
Completeness to theta = 25.60	99.5 %
Data / restraints / parameters	5167 / 71 / 421
Goodness-of-fit on F ²	1.079
Final R indices [I>2sigma(I)]	R1 = 0.0433, wR2 = 0.1109

$$R_1 = \frac{\sum ||F_o| - |F_c||}{\sum |F_o|}. \quad wR_2 = \frac{[\sum w(F_o^2 - F_c^2)^2 / \sum w(F_o^2)^2]^{0.5}}$$

Table S2. Crystal data and structure refinement for **3**.

Identification code	3
Empirical formula	C ₅₆ H ₄₆ CdCl ₂ N ₁₂ O ₁₁
Formula weight	1246.35
Temperature	100.01(10) K
Wavelength	0.71073 Å
Crystal system, space group	Tetragonal, <i>P4(3)2(1)2</i>
Unit cell dimensions	a = 15.89830(10) Å alpha = 90 deg. b = 15.89830(10) Å beta = 90 deg. c = 21.6675(7) Å gamma = 90 deg.
Volume	5476.59(18) Å ³
Z, Calculated density	4, 1.512 Mg/m ³
Absorption coefficient	0.570 mm ⁻¹
F(000)	2544
Crystal size	0.24 x 0.20 x 0.15 mm
Theta range for data collection	3.02 to 25.60 deg.

Reflections collected / unique	16691 / 5128 [R(int) = 0.0412]
Completeness to theta = 25.60	99.6 %
Data / restraints / parameters	5128 / 70 / 465
Goodness-of-fit on F ²	1.071
Final R indices [I>2sigma(I)]	R1 = 0.0417, wR2 = 0.0998

$$R_1 = \frac{\sum ||F_o| - |F_c||}{\sum |F_o|}. \quad wR_2 = \left[\frac{\sum w(F_o^2 - F_c^2)^2}{\sum w(F_o^2)^2} \right]^{0.5}$$

Table S3. Crystal data and structure refinement for **4**.

Identification code	4	
Empirical formula	C ₅₄ H _{41.2} CdCl ₂ N ₁₂ O ₁₀	
Formula weight	1201.50	
Temperature	100.03(11)K	
Wavelength	0.71073 Å	
Crystal system, space group	Tetragonal, <i>P</i> 41 21 2	
Unit cell dimensions	a = 15.90821(18) Å	alpha = 90 deg.
	b = 15.90821(18) Å	beta = 90 deg.
	c = 21.6184(4) Å	gamma = 90 deg.
Volume	5471.00(13) Å ³	
Z, Calculated density	4, 1.458 Mg/m ³	
Absorption coefficient	0.566mm ⁻¹	
F(000)	2444	
Crystal size	0.25 x 0.16 x 0.06 mm	
Theta range for data collection	3.18 to 25.60 deg.	
Reflections collected / unique	15884 / 5142 [R(int) = 0.0359]	
Completeness to theta = 25.60	99.5 %	
Data / restraints / parameters	5142 / 159 / 457	
Goodness-of-fit on F ²	1.074	
Final R indices [I>2sigma(I)]	R1 = 0.0447, wR2 = 0.1185	

$$R_1 = \frac{\sum ||F_o| - |F_c||}{\sum |F_o|}. \quad wR_2 = \left[\frac{\sum w(F_o^2 - F_c^2)^2}{\sum w(F_o^2)^2} \right]^{0.5}$$

Reference

(1) CrysAlisPro, Agilent Technologies, Version 1.171.36.32 (release 02-08-2013 CrysAlis171.NET) (compiled Aug 2 2013, 16:46:58).